

30
12/16/87 w.b. ①

UCID-21258

RESOLUTION LIMITATIONS AND OPTIMIZATION
OF THE ITT F4157 STREAK TUBE FOCUS
FOR FAST (10 ps) OPERATION

R. A. Lerche
E. L. Grasz
R. L. Griffith
R. A. Simpson
R. Posey

November 1987

Lawrence
Livermore
National
Laboratory

This is an informal report intended primarily for internal or limited external distribution. The opinions and conclusions stated are those of the author and may or may not be those of the Laboratory.
Work performed under the auspices of the U.S. Department of Energy by the Lawrence Livermore National Laboratory under Contract W-7405-Eng-48.

DISCLAIMER

This report was prepared as an account of work sponsored by an agency of the United States Government. Neither the United States Government nor any agency thereof, nor any of their employees, makes any warranty, express or implied, or assumes any legal liability or responsibility for the accuracy, completeness, or usefulness of any information, apparatus, product, or process disclosed, or represents that its use would not infringe privately owned rights. Reference herein to any specific commercial product, process, or service by trade name, trademark, manufacturer, or otherwise does not necessarily constitute or imply its endorsement, recommendation, or favoring by the United States Government or any agency thereof. The views and opinions of authors expressed herein do not necessarily state or reflect those of the United States Government or any agency thereof.

DISTRIBUTION OF THIS DOCUMENT IS UNLIMITED

RESOLUTION LIMITATIONS AND OPTIMIZATION OF THE ITT F4157
STREAK TUBE FOCUS FOR FAST (10 ps) OPERATION

UCID--21258

ABSTRACT

DE88 003727

The ITT F4157 image tube is biased at voltages far from the original design for operation in an ultrafast (10 ps) streak camera. Its output resolution at streak camera operating potentials has been measured as a function of input slit width, incident-light wavelength, and focus-grid voltage. The results are similar to those reported for the RCA C73435 streak tube. Indeed, the two tubes can be substituted for each other with minor mechanical modifications. The temporal resolution is insensitive to focus-grid voltage for a narrow (50 μm) input slit, but is very sensitive to focus-grid voltage for a wide (500 μm) input slit. Spatial resolution is nearly independent of focus-grid voltage for values that give good temporal resolution. Both temporal and spatial resolution depend on the incident-light wavelength. Streak camera operation is simulated with a computer program that calculates photoelectron trajectories. Electron ray tracing describes the observed effects of slit width, incident-light wavelength, and focus-grid voltage on the output resolution.

1. INTRODUCTION

Most streak cameras used by L-Division are of the EG&G design and incorporate either an ITT F4157 or RCA C73435 streak tube. These tubes are biased at their design voltages. Input to these cameras is typically via proximity coupled optical fibers with 50- μm core diameters. It has become increasingly important to improve the performance of these field cameras to

MASTER

S
DISTRIBUTION OF THIS DOCUMENT IS UNLIMITED

record signals with bandwidths greater than 5 GHz. The bandwidth of the present cameras is limited by the transit-time spread of the photoelectrons passing through the tube. In the Laser Program's ultrafast streak cameras, which use the RCA C73435 streak tube, the electric field strength at the photocathode surface is increased by rebiasing the tube far from the original design voltages.¹ This significantly reduces the electron transit-time spread.

The increased bandwidth requirement and knowledge of the RCA tube operating characteristics caused us to carefully examine the effect of slit width, focus-grid voltage, and incident-light wavelength on the ITT streak tube resolution under operating conditions similar to the Laser Program's streak camera. We used computer modeling, static measurements, and dynamic measurements to develop an understanding of the focusing properties of the ITT streak tube operating as a fast streak tube. An electron ray tracing computer program was used to model the streak tube operation. The results of the modeling helped establish the range of bias voltages used for our experimental measurements. The computer simulations predict the measured static characteristics and help us visualize the focusing properties of the tube. Static measurements adequately describe all of the focusing properties of the camera. They are used to predict the dynamic response of the camera to short (1 ps) laser pulses. An understanding of these focusing properties allows us to recognize the limitations of the tube and to optimize its resolution for specific applications.

2. TYPICAL STREAK CAMERA OPERATION

For this study, an ITT tube was placed in a standard Laser Program optical streak camera like the one shown schematically in Fig. 1. Incident light passes through band-pass and attenuating filters, then through a slit aperture. The slit is imaged onto the photocathode of the streak tube by a 1:1 relay lens. Emitted photoelectrons are accelerated and focused onto the tube's phosphor screen. Deflection plates sweep the image across the screen to provide a positional variation in intensity that corresponds to the time variation of the light intensity at the photocathode. A proximity focused microchannel plate (MCP) image intensifier tube (IIT) provides signal amplification for permanent recording with a CCD readout system.

2.1. BIAS VOLTAGE

The ITT F4157 tube is designed to operate as a streaked image tube.² It is cylindrically symmetric except for the gating grid (grid 1) and the deflection plates. The gating grid is a disk with a 2-mm by 30-mm slot spaced 7 mm from the photocathode. The tube was designed to operate with its gating grid, two focus grids (grids 2 and 3), and anode nominally set at the voltages listed in Table 1.³ Removal of the gating grid has no effect on the image quality of the tube because it follows an equipotential surface of the tube built without it. The cathode, focus grids, and anode form a spherical lens that images photoelectrons from the photocathode to the phosphor screen.

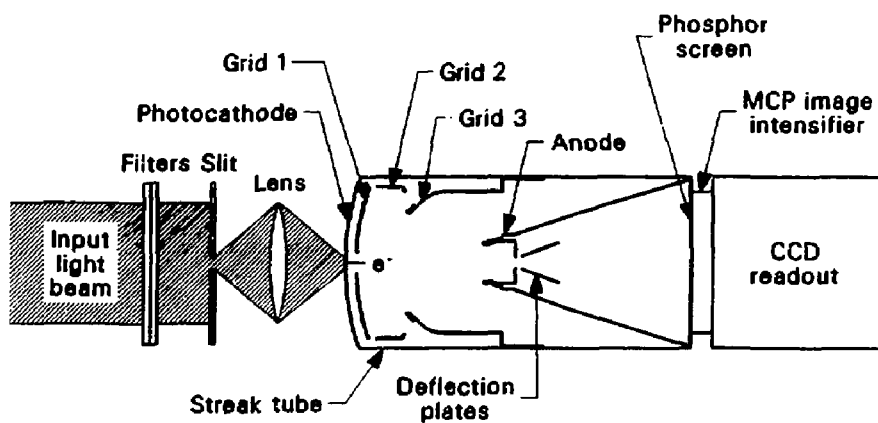


Figure 1. Schematic diagram of the streak camera.

Table 1. Nominal ITT F4157 image tube operating voltages.

Electrode	Streaked Image mode (volts)	Fast Streak Mode (volts)
Cathode	0	0
Grid 1 (gating grid)	150	2,250
Grid 2 (focus grid)	400	2,050
Grid 3 (focus grid)	1,600	900
Anode	15,000	15,000

Photoelectron transit-time spread through the tube limits the temporal resolution. It is inversely proportional to the electric field strength at the photocathode surface. For fast streak camera operation the extraction field is increased by applying a larger bias voltage between the gating grid and the photocathode. The gating grid now functions as an extraction grid. This destroys the axial symmetry of the electric field in the space around the extraction grid and forms a diverging, cylindrical lens for the photoelectrons.⁴ All photoelectrons except those originating in a narrow strip of the photocathode in the center of the slit are deflected away from their normal paths through the anode aperture. The focus grid potentials are adjusted to form the stronger positive lens required to focus the image of the input slit onto the phosphor screen. Typical bias voltages used in this camera are listed in Table 1. (All voltages in this paper are referenced to the photocathode.) Figure 2 shows selected equipotential lines near the gating grid for normal imaging and fast streaking operation.

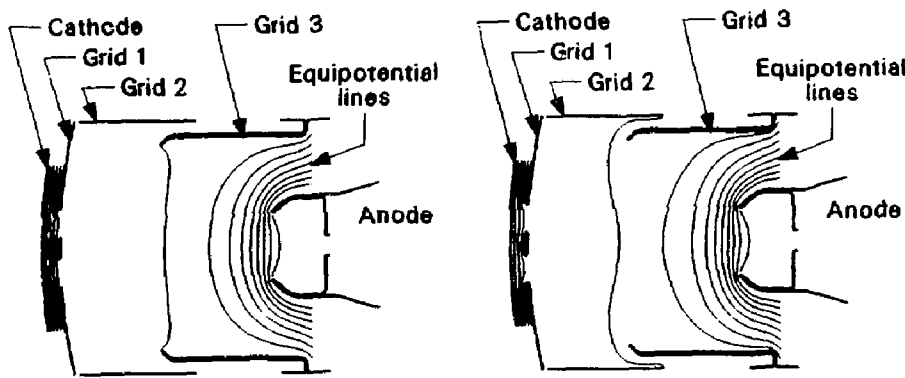


Figure 2. Plot of the equipotential lines in the region between the photocathode and the anode aperture. (a) shows streaked image mode operation with grid 1, grid 2, grid 3, and anode set at 0.15, 0.40, 1.6, and 15.0 kV, respectively. Equipotential lines are drawn at 30-volt intervals between the photocathode and grid 1, and at 1.5 kV intervals between grid 1 and the anode. (b) shows fast streak mode operation with grid 1, grid 2, grid 3, and the anode set at 2.25, 2.05, 0.9, and 15.0 kV, respectively. Equipotential lines are drawn at 500 volt intervals between the photocathode and grid 1, and at 1.5 kV intervals between grid 1 and the anode. Note the cylindrical lens formed near grid 1.

2.2. STREAK CAMERA PREPARATION

The ITT tube used in this work has a fiber optic input plate and an S20 photocathode. To fit it into the Laser Program's streak camera required two minor mechanical modifications: a slight enlargement of the hole in the back plate and the addition of spacers between the front plate and the relay lens. For static characterization of the camera with the ITT tube, three separate, variable power supplies were used to bias the three grids. Grid voltages were monitored with electrostatic voltmeters. For dynamic measurements, the streak camera was operated with its normal high voltage supply and deflection circuit. Since the normal power supply has provisions for biasing only one focus grid and focusing is found to be insensitive to the voltage applied to grid 2, grid 2 was connected to grid 1.

3. STREAK TUBE FOCUSING PROPERTIES

Work to determine the focusing properties of the ITT streak tube was done in three distinct stages: static measurements, dynamic measurements, and computer modeling. Static characterization refers to measurements taken while the streak camera is operating in its "pulsed" mode with the deflection plates grounded. Static characterization is much easier to perform than dynamic characterization. Its purpose is to predict the dynamic response (temporal resolution, spatial resolution, and onset of saturation) of the streak camera under nearly ideal conditions. The camera operates at its normal voltages with the IIT gated for 100 μ s. The output image can be formed with input power that varies by several orders of magnitude and the output image shape is independent of the input temporal

shape. The experimental setup used for static characterization is shown in Fig. 1. For the static resolution measurements reported in this paper, the light source is an incandescent lamp with the appropriate band-pass filter. A CCD readout was used to enable rapid data analysis.

3.1. TEMPORAL RESOLUTION

Four factors determine the temporal resolution of a streak camera: static image width, sweep speed, photoelectron energy spread, and extraction field strength. The image width Δx and the sweep speed S of the image along the temporal axis at the output of the tube determine the focus-limited temporal response Δt_x which may be written as

$$\Delta t_x = \Delta x / S . \quad (1)$$

The energy spread of photoelectrons simultaneously emitted from the photocathode results in a temporal spread in their arrival times at the phosphor screen. The extent of this transit-time spread Δt_t depends on the electric field strength E at the photocathode surface and the energy spread of the photoelectrons Δe . For our cameras most of the transit-time spread occurs while the electrons are near the photocathode and may be written as

$$\Delta t_t = 3.37 \times 10^{-8} \sqrt{\Delta e} / E . \quad (2)$$

where Δt_t is in seconds, Δe in eV, and E in volts/cm. The overall time response of the tube is the focus-limited response added in quadrature with the transit-time spread, that is

$$\Delta t = [(\Delta t_x)^2 + (\Delta t_t)^2]^{1/2} \quad (3)$$

Responses reported in this paper are given as full-width at half-maximum (FWHM) values.

The focus-limited temporal response of a streak camera can be estimated from the static image width and sweep speed using Eq. (1). Figure 3 shows a typical set of data plotted as a function of two variables: input slit width and streak tube focus-grid (grid 3) voltage. The sensitivity of the image width to focus voltage differs greatly for the two slit widths. The image width of the 50- μm slit is relatively insensitive to the focus voltage while the image width of the 500- μm slit is very sensitive to it. At the optimum wide slit focus voltage, the image width is insensitive to input slit width. Data were recorded for grid 2 voltages in the range between 1,450 and 2,500 volts. For both slit widths the static image width is insensitive to the voltage applied to the grid 2. Figure 4 shows data recorded with grid 2 voltages of 1,450 and 2,250 volts. It is the insensitivity to the voltage applied to grid 2 that allows grid 1 and grid 2 to operate at the same potential without affecting the temporal performance.

The dynamic response of a camera can be predicted from static data like that shown in Fig. 3. It can be determined by measuring its response to a very short pulse. Measurements were made using 1-ps, 0.605- μm dye laser

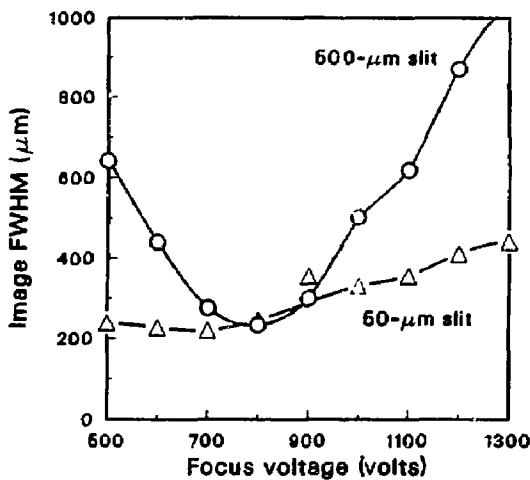


Figure 3. Static image width along the temporal axis versus focus-grid (grid 3) voltage for 800- μm light. Data are presented for 500- μm and 50- μm slits. The streak tube has an S20 photocathode.

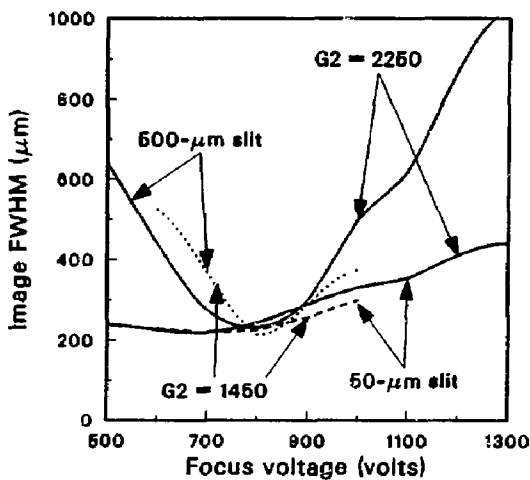


Figure 4. Measured image width as a function of focus-grid (grid 3) voltage for grid 2 voltages of 1,450 volts and 2,250 volts. The optimum operating point is insensitive to the grid 2 voltage.

pulses passed through an etalon to produce a set of pulses spaced 296 ps apart. Figure 5 shows the dynamic pulse width plotted with the predicted temporal response based on the 0.8- μm data shown in Fig. 3 and the sweep speed value determined from the dynamic data. These predictions include the effect of a 9-ps transit-time spread estimated from the electric field strength at the photocathode and an axial photoelectron energy spread of 0.5 eV.

3.2. SPATIAL RESOLUTION

One way to determine the camera's spatial resolution is to measure its point spread function (PSF). Using static measurements, the PSF was formed by illuminating a 50- μm by 50- μm square aperture with a low intensity light source. The resulting image width, taken perpendicular to the sweep direction, is the spatial resolution of the camera. The spatial image width plotted as a function of the focus-grid voltage (grid 3) is shown in Fig. 6 for 0.8- μm and 0.45- μm light. The data shows the spatial image width to be insensitive to the focus voltage. Other data show the spatial resolution to be insensitive to the voltage applied to grid 2.

Computer simulation of the streak tube operation show that the spatial resolution of the tube depends on the initial transverse energy distribution of the photoelectrons. The greater the energy the poorer the resolution. Poorer resolution is expected for the shorter wavelength light because the energy available to a photoelectron leaving the photocathode surface is the difference between the incident photon energy and the work function of the surface.

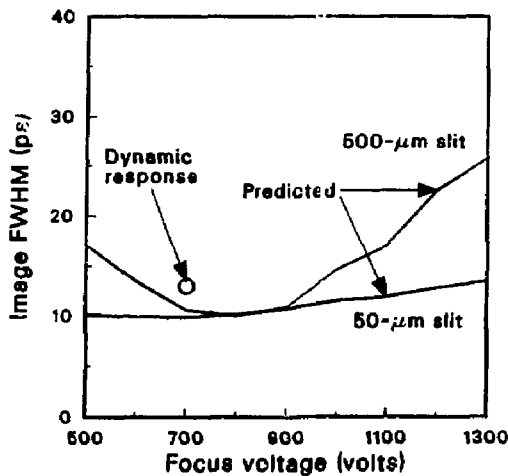


Figure 5. Measured and predicted temporal resolution. The data point represents a dynamic measurement. The solid lines represent predictions based on the data presented in Fig. 3.

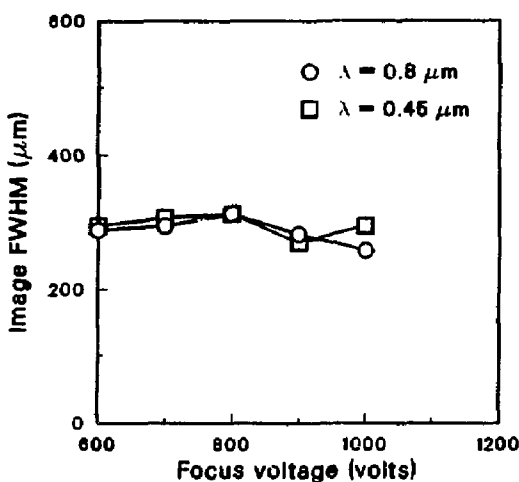


Figure 6. Streak camera spatial resolution versus focus-grid voltage for 0.80-μm and 0.45-μm light.

A dependence of spatial resolution on photon wavelength was clearly observed for an RCA tube with an S1 photocathode. It is possible that these measurements for the ITT tube are limited by the focusing of the image onto the photocathode surface, and thus represent a worst case measurement. Data recently reported for a Thompson 506 streak camera using the ITT tube show a spatial resolution around 150 μm for 0.6- μm light.⁵

4. MODELING STREAK CAMERA OPERATION

The streak tube operation was simulated with a computer program to predict the static operating characteristics of the tube and to determine bias conditions which might give the resolution and bandwidth needed for the high-bandwidth project. The modeling shows that the ITT and the RCA tubes operate in a similar manner and have similar characteristics.

A modified version of Herrmannfeldt's electron trajectory computer program⁶ was used to model the effects of slit width, focus-grid voltage, and photoelectron energy on the streak tube resolution. Effects due to space charge and magnetic fields were not investigated. Input to the program consists of electrode boundary conditions and initial conditions for selected electron trajectories. Graphic and tabular output includes electrode profiles, equipotential lines, electron trajectories, and electron transit times to the phosphor screen. To reduce computational time needed to run the simulations, a few carefully selected trajectories are used to represent the spatial and energy distributions of the photoelectrons emitted from the photocathode.

The program allows the use of either cylindrical or rectangular symmetry, but not both. The image tube in streaked operation has rectangular symmetry between the cathode and extraction grid and makes a transition to cylindrical symmetry between the extraction grid and the focus grid. To model tube operation, the extraction grid opening is modeled as a 7-mm wide ring with a 5-mm inner diameter. The electric field distribution across the ring is nearly identical to that across a rectangular slot of equal width. The electric field after the extraction grid is virtually unaffected by the modeling of the slot. The analysis of the temporal and spatial focusing properties of the tube are treated as separate problems.

4.1. FOCUS-LIMITED TEMPORAL RESPONSE

For calculating the focus-limited image width parallel to the streak direction, the slit width is modeled by the starting coordinates of the selected electron trajectories. Trajectories starting from a single point on the photocathode simulate illumination through a narrow slit or fiber. Trajectories starting from a set of equally spaced points along the photocathode surface simulate illumination through a wide slit. See Figs. 7 and 8.

The velocity distribution of the photoelectrons emitted from the photocathode depend on the incident photon energy and the photocathode material. The image width in the temporal direction depends on the initial transverse velocity distribution of the photoelectrons, while the transit-time spread between the photocathode and phosphor screen depends on the

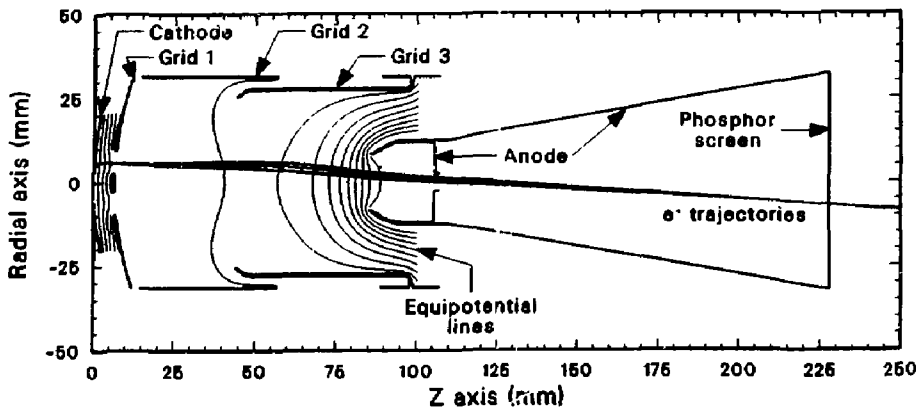


Figure 7. Electron trajectories for a narrow slit simulation of streak tube operation. The plot shows selected electron trajectories, equipotential lines, and electrode profiles. The trajectories start from a single point on the photocathode with different amounts of transverse energy. The extraction grid, the two focus grids, and anode are biased at 2.25, 2.05, 0.7, and 15 kV, respectively. Trajectories are plotted for initial transverse electron energies of 0, 0.125, and 0.25 eV.

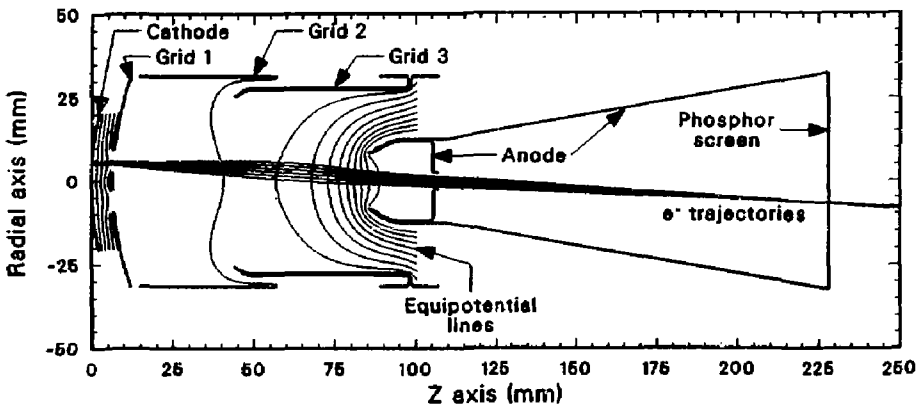


Figure 8. Electron trajectories for a wide slit simulation of streak tube operation. The plot shows selected electron trajectories, equipotential lines, and electrode profiles. The trajectories start from points uniformly spaced across the photocathode. The extraction grid, focus-grids, and anode are biased at 2.25, 2.05, 0.825, and 15 kV, respectively. Trajectories are plotted for 0 eV electrons. Spacing between trajectory starting points is 200 μ m.

initial axial velocity distribution of the photoelectrons. Four trajectories from each starting point are used to model the velocity distributions. The transverse velocity distribution is modeled by two electrons having equal energies but in opposite directions parallel to the photocathode surface. The axial velocity distribution is modeled by one electron with no initial energy and one with an axial energy equal to 70 percent of the photon energy above the photocathode work function.

Figure 7 shows electron trajectories that simulate the photocathode being illuminated through a narrow slit by light of several different wavelengths. The electrons emitted with different tangential energies focus to an image plane that coincides with the plane of the phosphor screen when the focus grid voltage is 1,000 volts. The image plane moves toward the photocathode for lower voltages and further away for larger voltages. Figure 9 shows the image width at the screen plotted as a function of focus-grid voltage for the transverse energies of 0.03 eV and 0.125 eV. The optimum focus voltage is independent of the incident light wavelength. The image width is also independent of wavelength at the optimum focus grid voltage. The slope of each curve away from the optimum focus voltage depends on the initial transverse energy distribution of the electrons. Greater transverse energy causes a greater slope.

The electron trajectories shown in Fig. 8 simulate the photocathode being illuminated through a wide slit by photons with an energy equal to the work function of the photocathode. Only trajectories starting from about a 1.5-mm wide strip of the photocathode centered relative to the extraction-grid slot pass through the anode aperture to the phosphor screen. The

electrons emitted from points within this wide strip converge at a plane that coincides with the phosphor screen for a focus-grid voltage near 1,100 volts. The focal point moves toward the photocathode for lower voltages and further away for higher voltages. Figure 10 shows the image width of the wide slit plotted as a function of focus-grid voltage for transverse energies of 0 eV. The image width shows a strong dependence on focus-grid voltage and has a minimum at 1,100 volts.

4.2. SPATIAL RESOLUTION

The voltage applied to the extraction grid forms a cylindrical lens. Note that there is no transverse electric field perpendicular to the sweep direction in the space between the photocathode and extraction grid. Simulation of the spatial focusing is done by assuming the extraction grid is a fine mesh biased at a constant potential. Electron ray tracing shows that the spherical lens formed by the focus grid and anode is too weak to focus the photoelectrons in the spatial direction. The output spot size increases with increasing transverse energy of the photoelectrons. With the extraction grid voltage set at 2,250 volts, the image width appears to be independent of the focus-grid voltage (grid 3) for values between 500 and 1,100 volts.

5. SUMMARY

The focusing properties of the ITT F4157 image tube operating as a fast streak tube are presented. They were measured using static techniques and include the dependence of temporal and spatial resolution on input slit

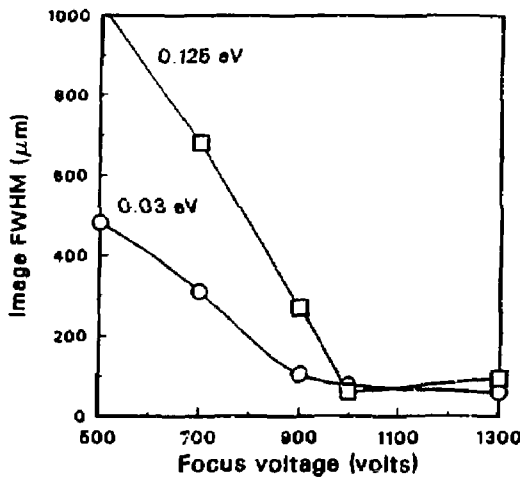


Figure 9. The focus-limited image width (temporal axis) versus focus-grid voltage for narrow slit operation predicted using electron trajectory calculations. Curves are presented for average transverse electron energy distributions of 0.03 and 0.125 eV.

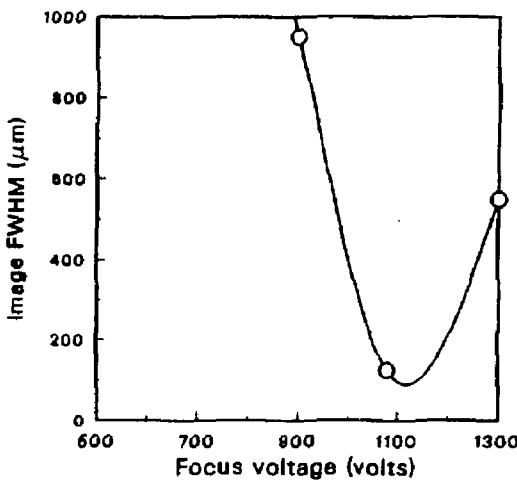


Figure 10. The focus-limited image width (temporal axis) versus focus-grid voltage for wide slit operation predicted using electron trajectory calculations. The curve presented is for the average transverse electron energy distribution of 0.0 eV.

width, incident-photon energy, and focus-grid voltage. The static data are used to accurately predict the measured dynamic response of the camera to a 1-ps laser pulse. Simulation of streak tube operation using an electron ray tracing program is described. The simulations predict and explain the major features of the static characteristics.

For the bias voltages used on the streak tube, the temporal resolution is found to be insensitive to slit width. Temporal resolution is also relatively insensitive to focus voltage for a narrow slit, but not for wide slit. The spatial resolution at focus-grid voltages producing reasonable temporal focusing is nearly independent of the focus-grid voltage. Both temporal and spatial resolution depend on the incident-light wavelength.

Streak camera operation is modeled with a computer program that calculates photoelectron trajectories. Simulations using selected electron trajectories describe all of the observed effects of slit width, incident-light wavelength, and focus-grid voltage on the output image width. The focus-grid voltage controls the axial position of best temporal focus. It coincides with the phosphor screen at focus-grid values of 1,100 volts for a wide slit and 1,000 volts for a narrow slit. Lower voltages form a stronger electrostatic lens and move the image plane towards the photo-cathode. The temporal image width depends on the initial transverse energy of the photoelectrons parallel to the sweep axis of the tube while the spatial image width depends on the transverse energy perpendicular to the sweep axis of the tube.

6. ACKNOWLEDGMENTS

The authors would like to thank M. Lowry for the use of the ITT streak tube used for this project, and N. Landen for his assistance at the Short Pulse Laser Facility. We also thank R. Floryan of ITT for supplying us with the F4157 electrode shapes needed for modeling the tube operation.

7. REFERENCES

1. R. A. Lerche and R. L. Griffith, Resolution Limitations and Optimizations of the LLNL Streak Camera Focus, to be published in Conf. on High Speed Photography, Videography, and Photonics V, SPIE Proc. 832, (1987). Also UCRL 96519 (1987).
2. ITT specification sheet for the F4157 streak tube.
3. C. C. Lai and L. B. Olk, Performance Characterization of an Image Converter Based Streak Camera, Conf. on High Speed Photography, Videography, and Photonics III, SPIE Proc. Vol. 569 (1985). Also LLNL report, UCRL-92214, (1985).
4. R. G. Stoudenheimer, Ultra-High Speed Streak Photography Using Image Tubes, RCA Application note AN-4789 (1971).

5. M. Lowry, G. Lancaster, D. Jander, E. Grasz, R. Simpson, B. Rickard, C. Imhoff, and R. Lerche, Characterization of a Large-Format, High-Fidelity Picosecond, Optical Streak Camera, to be published in Conf. on High Speed Photography, Videography, and Photonics V, SPIE Proc. 832, (1987). Also LLNL report, UCRL 96920.
6. W. B. Herrmannfeldt, Electron Trajectory Program, Stanford Linear Accelerator Center, Stanford, California, SLAC-Report-226 (1979).